# Numerical Simulation of Cross-Valley Plume Dispersion during the Morning Transition Period*

DAVID C. BADER AND C. DAVID WHITEMAN

*Pacific Northwest Laboratory, Richland, Washington*

(Manuscript received 2 June 1988, in final form 7 November 1988)

ABSTRACT

A two-dimensional dynamical model was used to simulate the daytime boundary-layer evolution and resulting plume dispersion in a cross-valley section of a northwest–southeast oriented narrow valley in the first 4 h after sunrise. Two cases were simulated, one using a summertime heating distribution and a second with a wintertime heating distribution. In each case, additional conservation equations were added to simulate the dispersion of two plumes released 150 m and 650 m above the valley floor. In the summer case, the lower plume migrated to the more strongly heated southwest sidewall in the first 90 min after sunrise, and was then advected up the sidewall in the slope flow for the remainder of the simulation. This result is consistent with observations. The upper plume diffused slowly in the remnants of the nocturnal inversion layer until it was entrained by the growing convective boundary layer 3 h after sunrise. The boundary layer's thermodynamic structure remained nearly symmetric about the valley axis throughout the transition period. The asymmetric dispersion characteristics seen in the summer case were not found in the winter simulation. The seasonal change in solar illumination reduced the differences in sufrace heat flux between the two sidewalls that gave rise to the asymmetry observed in the summer case.

## 1. Introduction

The destruction of the nocturnal inversion layer that typically fills a mountain valley at sunrise has important air pollution implications. Pollutant material released into this layer usually remains trapped in the stable air mass until the inversion is destroyed after sunrise, at which time it is released into the large scale flow field above the valley. Furthermore, ground-level concentrations of pollutants emanating from elevated sources can rapidly increase during morning fumigation episodes within the valley. Previously, Whiteman and Allwine (1985) developed a dispersion model for the morning transition period in narrow valleys that was based on Whiteman and McKee's (1982) thermodynamic formulation of Whiteman's (1982) conceptual model of inversion destruction. According to the conceptual model, the nocturnal inversion is destroyed by two processes. One is the growth of a convective boundary layer (CBL) along the valley floor and sidewalls and the second is the heating and removal of air from the CBL beneath the stable layer to the region above the valley by the slope winds. The latter mechanism results in the abdiabatic descent of the stable layer within the valley as the morning transition proceeds.

Subsequently, Bader and McKee (1983, 1985) used a dynamical model to study the cross-valley development of the daytime boundary layer in narrow mountain valleys. Their results were in basic agreement with Whiteman's (1982) conceptual model with two important additions. First, the recirculation of air over the sidewalls into the stable air mass was identified as a third process contributing to inversion destruction. Second, the model results revealed that cross-valley mixing and gravity wave motions rapidly compensated for differences in surface heating rates between the two opposite sidewalls. Consequently, no large asymmetries were able to develop in the valley boundary layer's thermodynamic structure. However the results from a tracer experiment conducted in the Brush Creek Valley in Colorado (Whiteman 1989) raised some questions about the validity of these results. That experiment revealed a pronounced asymmetry in the mass flow field when the differences in heating between the opposing sidewalls were large. In this paper, the dynamical model is used to examine the relationship between surface heat flux distribution and pollutant dispersion in a cross-valley section during the morning transition period. The results from the simulations will be compared to the field observations. The effects of plume elevation and season will also be studied to determine their importance on dispersion during the morning boundary layer evolution.

* Work supported by the U.S. Department of Energy under Contract DE-AC06-76RLO 1830.

*Corresponding author address:* David C. Bader, Atmospheric Sciences Department, K6-08, Battelle Pacific Northwest Laboratory, P.O. Box 999, Richland, WA 99352.

## 2. Review of tracer experiment

Figure 1 presents two analyses of plume concentrations on a vertical cross section of Colorado's Brush Creek Valley during the morning transition period of 4 August 1982. More complete information can be found in the accompanying paper by Whiteman (1989). The vertical cross section of the valley is drawn through a location 7.7 km down the sloping valley floor from the tracer release site. At the release site (1922 m MSL), sulfur hexafluoride was released continuously from an altitude of 2027 m MSL beginning at 0428 LST using a tethered balloon release system. Since the base of the cross section in Fig. 1 is at 1780 m MSL, the tracer plume was released 247 m above the base of the cross section. Data in the figure are a composite of available data from surface, balloon-borne and aircraft sampling systems. Astronomical sunrise was at 0504 LST and sunlight progressed slowly down the southwest sidewall, producing local sunrise at the valley center at 0643 LST.

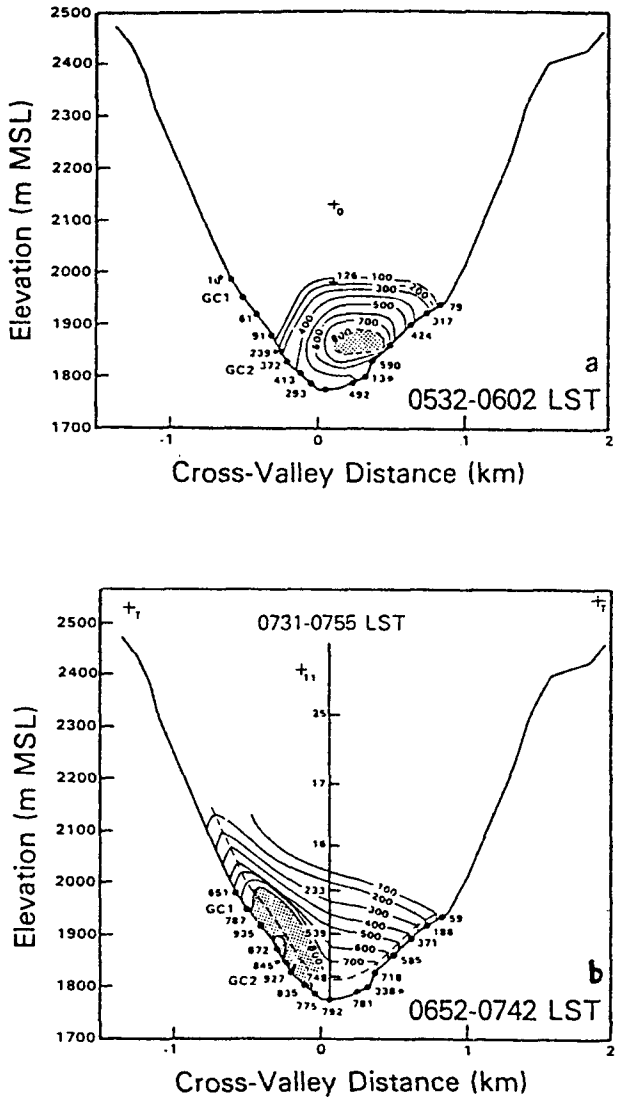


FIG. 1. Vertical cross sections of Colorado's Brush Creek Valley showing the transport and dispersion of an elevated sulfur hexafluoride plume during the morning transition period on 4 August 1984. The sampling times for the surface-based samplers are shown in the lower right corner of each subfigure. The cross sections run from southwest (left) to northeast (right). Contours in parts per trillion. (a) Presunrise plume, and (b) concentrations after sunrise when the southwest sidewall was strongly illuminated by the sun. The dashed line indicates an estimated convective boundary layer height. GC1 and GC2 are sites where portable gas chromatographs were operated. Concentrations indicated with an asterisk in the figure indicate questionable low volume samples that were not used in analysis. In Panel (b), the sampling time for the balloon-borne sampler is indicated at the top of the vertical profile. See text and Whiteman (1989) for further information.

The nocturnal tracer plume (Fig. 1a) was carried down the valley to the cross section, traveling adjacent to the northeast sidewall in the lowest 200 or 300 m of the valley. The mean plume centerline on the cross section was generally found about 100 to 150 m above the valley floor, indicating that the nocturnal plume traveled in a path nearly parallel to the valley floor, rather than maintaining a constant MSL height. The plume centerline concentration was greater than 800 ppt on the cross section. As sunlight progressed down the southwest sidewall a cross-valley flow developed, advecting the tracer plume toward the sunny sidewall (Figure 1b). High concentrations occurred on the southwest sidewall as the nocturnal plume was entrained into a growing convective boundary layer (CBL), fumigating the surface. Upslope flows in the growing CBL carried the tracer farther up the sidewall, increasing concentrations in the upper regions of the valley. After 0730 LST the along-valley wind reversal (to up-valley) was an additional factor that caused a rapid diminution in concentrations within the lower half of the valley.

## 3. Model description

The model is a modified and updated two-dimensional version of the Colorado State University Cloud/Mesoscale Model (Tripoli and Cotton 1982) that was used for the earlier studies. The most significant improvement over the earlier version for complex terrain boundary layer simulations is the inclusion of Yamada's (1983) prognostic turbulent kinetic energy (TKE) formulation to evaluate the turbulent fluxes. A quasi-Boussinesq, elastic primitive equation set is employed on a terrain following coordinate system to predict wind components, potential temperature, pressure, subgrid scale TKE, the product of TKE and the turbulent length scale, and an arbitrary number of passive tracer concentrations. Temperature and density are diagnosed from the predicted quantities. Turbulent fluxes are calculated using a K-theory closure in which the eddy mixing coefficients are diagnosed from the local stability, turbulent length scale and TKE. A time-split

integration scheme is used to solve the equations numerically on a staggered grid mesh. Bader et al. (1987) describe the current model in more detail.

The model domain is an idealized cross section of the Brush Creek Valley at the location of the tracer sampling arc (Fig. 2). Vertical grid spacing was 50 m in the lowest 15 levels above the surface with an additional 17 levels included on a telescoping grid below the horizontal model top located 3 km above the valley floor. The coordinate transform (Clark 1977) slightly reduced the grid spacing above the elevated sections of the terrain. Total interior model domain width was 7.9 km divided into equidistant grid columns 100 m apart. The slope of the valley sidewalls was constant at 0.4 and ended in flat ridges 700 m above the 1-km-wide valley floor. Lateral boundary conditions modified the Orlanski (1976) radiation boundary condition at the interior model domain boundaries with the mesoscale adjustment procedure described by Tripoli and Cotton (1982). In this configuration, there is no flow through the outside Mesoscale Compensation Region (MCR) boundaries. The MCR's are single columns of grid boxes that are as wide as the interior domain and are added to control mass loss trends resulting from outflow circulations at the interior domain boundaries. The gravity wave radiation boundary condition described by Klemp and Durran (1983) was used at the model top, although tests with a rigid lid revealed no significant differences since the strong boundary layer circulations developed in the lowest 1 km above the surface.

The surface layer parameterization was adapted from a formulation by Louis (1979) based on the flux-profile relationships developed by Businger et al. (1971). Surface friction velocity is computed for the lowest grid boxes based on the velocity and a specified surface kinematic heat flux. The surface heat flux was calculated to be 20% of the incident extraterrestrial solar radiation at each surface point according to the formulas given by Revfeim (1976). A zero heat flux was assumed on shaded areas. In reality, these regions would probably be cooling the overlying air. The magnitude of the cooling compared to the intensity of the heating above the illuminated locations, however, makes this effect negligible for the purposes of this study. Solar zenith angle, aspect and orientation definitions assumed that the model valley was located at 40°N and that the valley lies on a northwest–southeast axis, approximately the characteristics of the Brush Creek Valley. Conditions on two different days were modeled, the summer and winter solstices, to contrast the effects of the different seasonal heat flux distributions on dispersion and boundary layer development in the valley. Although there were no initial or external winds specified for the model experiments, the turbulent effects of a 2 m $s^{-1}$ along-valley wind were included in the surface layer.

Figure 3 shows the initial plume and potential temperature structure in the valley for both simulations

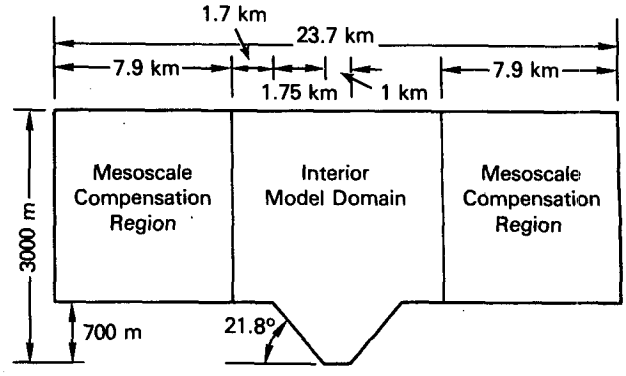


FIG. 2. Model domain (not to scale).

(the vertical coordinate has been exaggerated 3.5 times with respect to the horizontal). The model atmosphere was initialized with an 8.25 K potential temperature inversion from the floor to 125 m above the valley bottom. Overlying the low-level inversion was a deep isothermal layer ($d\theta/dz = 0.01$ K $m^{-1}$) that extended to 1100 m AGL. A free atmosphere layer with a lapse rate of 0.004 K $m^{-1}$ filled the model domain from 1100 m AGL to the top. This sounding is typical of those observed at sunrise in the Brush Creek Valley during the 1982 and 1984 field experiments conducted by the U.S. Department of Energy's Atmospheric Studies in Complex Terrain (ASCOT) program. Two circular plumes with Gaussian concentration distributions were located above the valley axis with centerlines at 150 m AGL and 650 m AGL. The lower plume was an idealized representation of the observed tracer plume at sunrise while the upper plume was added to examine dispersion in the elevated isothermal layer. Plume concentrations in both cases were normalized by the initial centerline value and no tracer material was added after the start of the simulation. This state marked model "sunrise" at which time surface heating was initiated. The model runs were continued for 4 h simulated time with instantaneous fields saved at 15 min intervals on computer file.

## 4. Results

### *a. Summer case results*

In this simulation, the solar geometry is such that the northeast sidewall remains shaded for 90 min after sunrise while the southwest sidewall is strongly illuminated. Figure 4a shows the summer simulation fields 60 min after sunrise. The stable "core" region of the valley is enclosed by the outer broken line and marks the area where the lapse rate exceeds 0.008 K $m^{-1}$. The inner broken line shows the strongly stable inversion region in the bottom of the valley where $d\theta/dz$ exceeds 0.016 K $m^{-1}$. At this time, the northeast sidewall is still shaded, but weak surface heating has produced a shallow mixed layer along the upper two-thirds of the

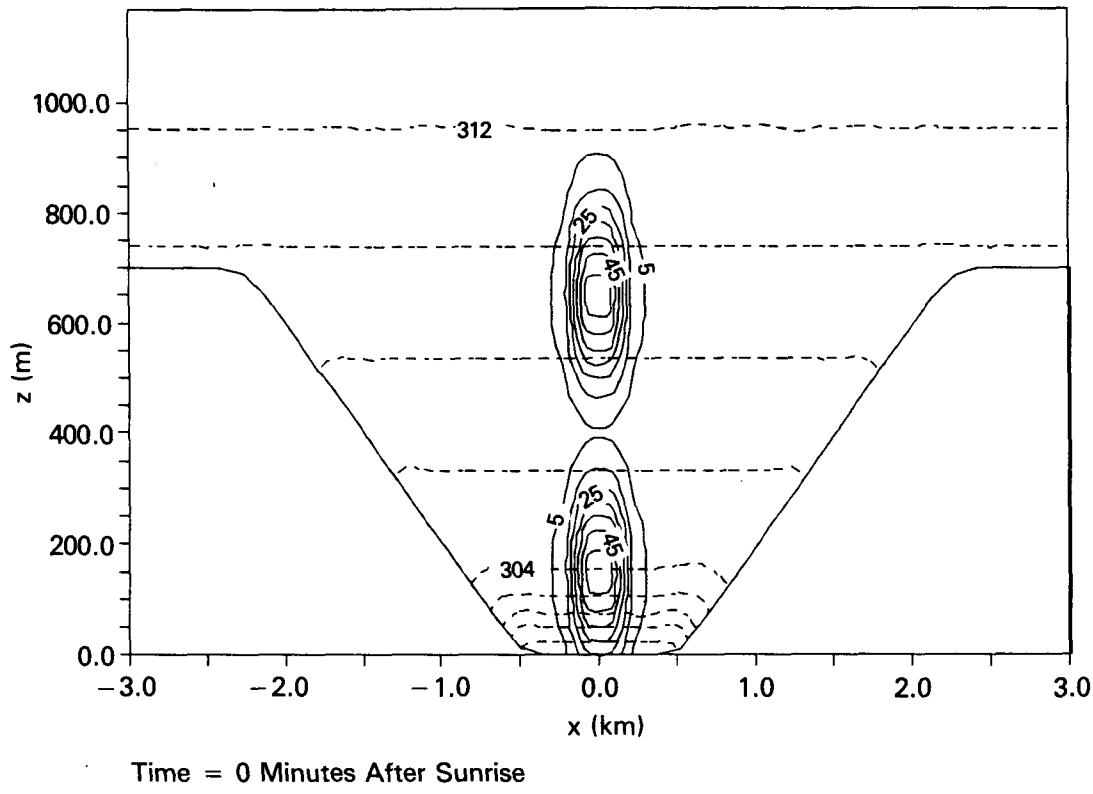


FIG. 3. Initial plume and potential temperature structure for both simulations. Potential temperature contour interval is 2 K (dashed lines). Plume concentration contour interval is 10%.

southwest sidewall. Weak motions in the stable core have started to distort the plumes and a slight movement of the lower plume toward the heated sidewall can be discerned. Weak slope winds with speeds less than 0.5 m $s^{-1}$ developed over the upper part of the southwest sidewall, but they did not extend over the entire sidewall length. Weak and variable winds appeared over the shaded northeast sidewall and in the valley center in response to the dynamic disturbances induced by the heating over the illuminated floor and southwest side.

By 90 min after sunrise (Fig. 4b), the northeast sidewall is no longer shaded and weak slope winds have developed near the sidewall summit. The lower plume diffused and shifted toward the strongly heated southwest sidewall, while the upper plume diffused slowly in the stable core above the valley axis. The outline of the stable core displays the characteristic pattern of alternating regions of strong and weak stability over the sidewalls that was seen in the earlier modeling studies. Near-neutral regions result from cross-valley wind convergence zones, while a divergence region forms farther up the sidewall. The net effect of this structure is to enhance the cross-valley mixing and gravity wave processes that destabilize the inversion layer. Figure 5 shows the corresponding wind and potential temperature structure. The slope winds over both sidewalls are turbulent and discontinuous with 1.5–2.0 m $s^{-1}$ thermal circulations directed toward the lateral domain boundaries above ridgetop. As was found in the earlier studies, the boundary layer's thermal structure remains nearly symmetric about the valley axis, although the mean mass flow field shown by the tracer is obviously distributed asymmetrically in the valley's lower half.

Figure 4c displays the stable core and tracer positions 120 min after sunrise. The stronger midmorning surface heating has intensified the slope circulations and advected tracer material from the lower plume up the southwest sidewall. Wind speeds over the upper sidewall were near 2.0 m $s^{-1}$ and some tracer material was being vented into the neutral layer overlying the valley, although the concentrations were just 0.5–1.0% of the initial centerline values. Also evident was the enhanced cross-valley dispersion of material in the upper plume that resulted from the increased cross-valley mixing. The elevation of the upper plume centerline has lowered nearly 50 m and the top of the stable layer has a concave upward shape, indicating the mean descent of the layer.

An hour later (Fig. 4d and 4e), CBL growth dominates the morning transition processes. The lower plume tracer is carried up the southwest sidewall in the 1.0–2.0 m $s^{-1}$ slope wind and vented to the layer

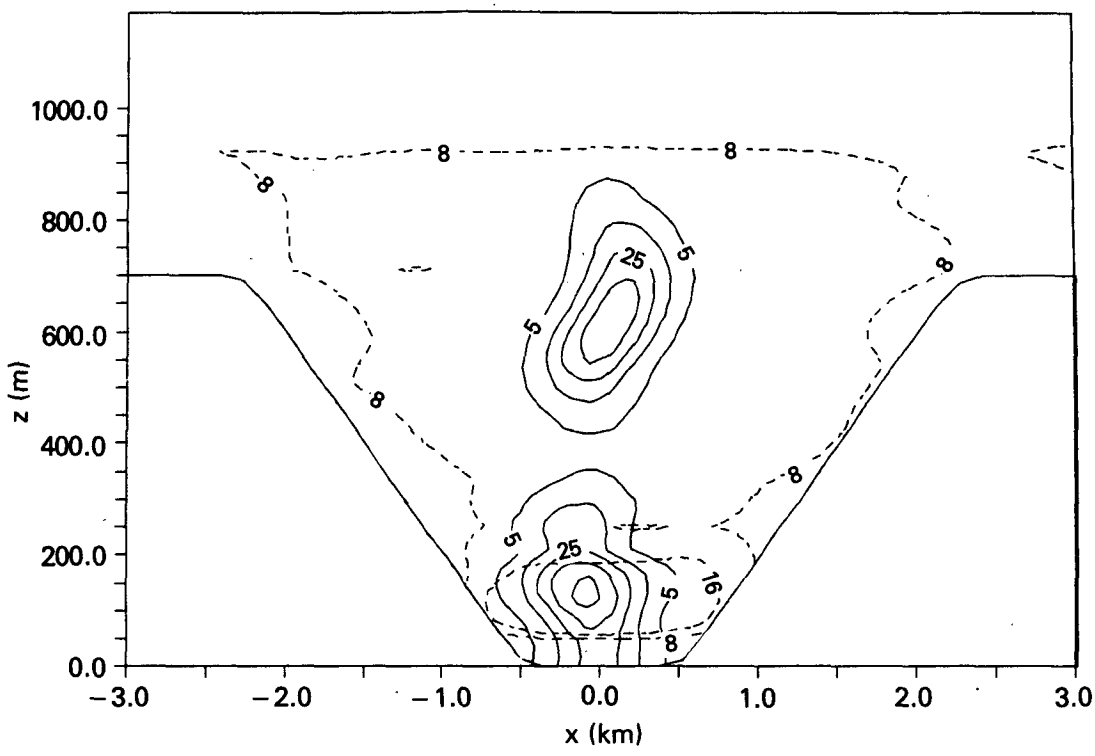


Time = 60 Minutes After Sunrise

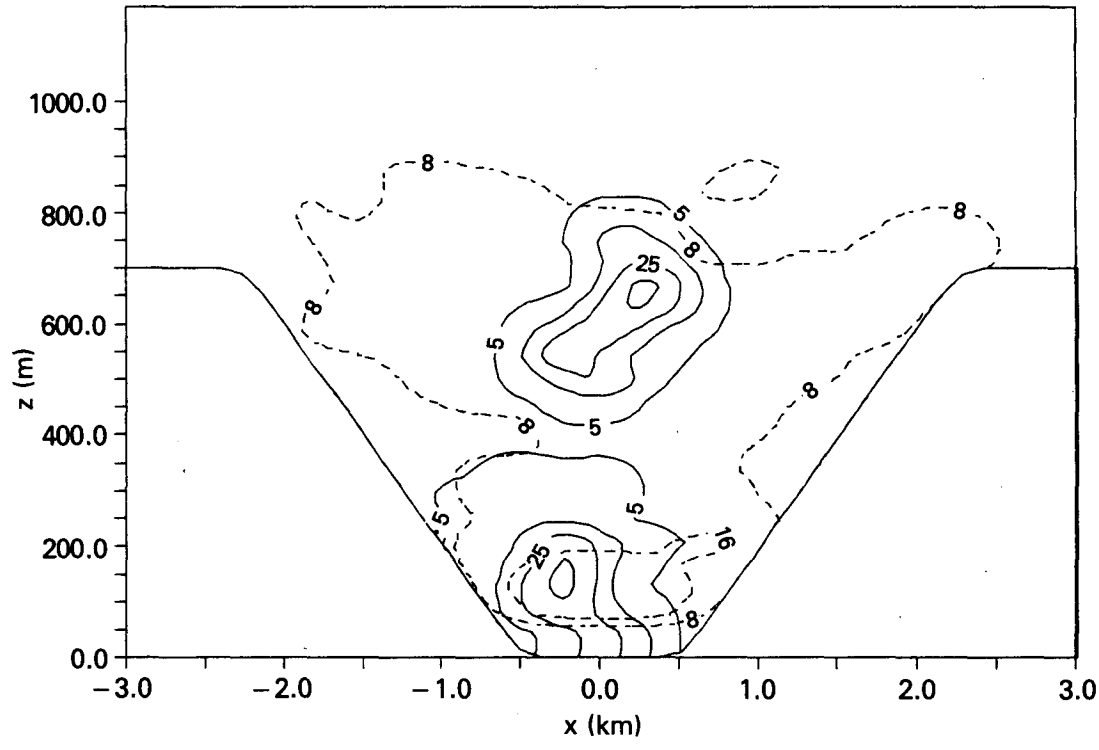


Time = 90 Minutes After Sunrise

FIG. 4. Plume structure (solid contours) and lapse rate (dashed contours) for summer case after (a) 60 min, (b) 90 min, (c) 120 min, and (d) 180 min for lower plume, (e) 180 min for upper plume, (f) 240 min for lower plume, and (g) 240 min for upper plume.

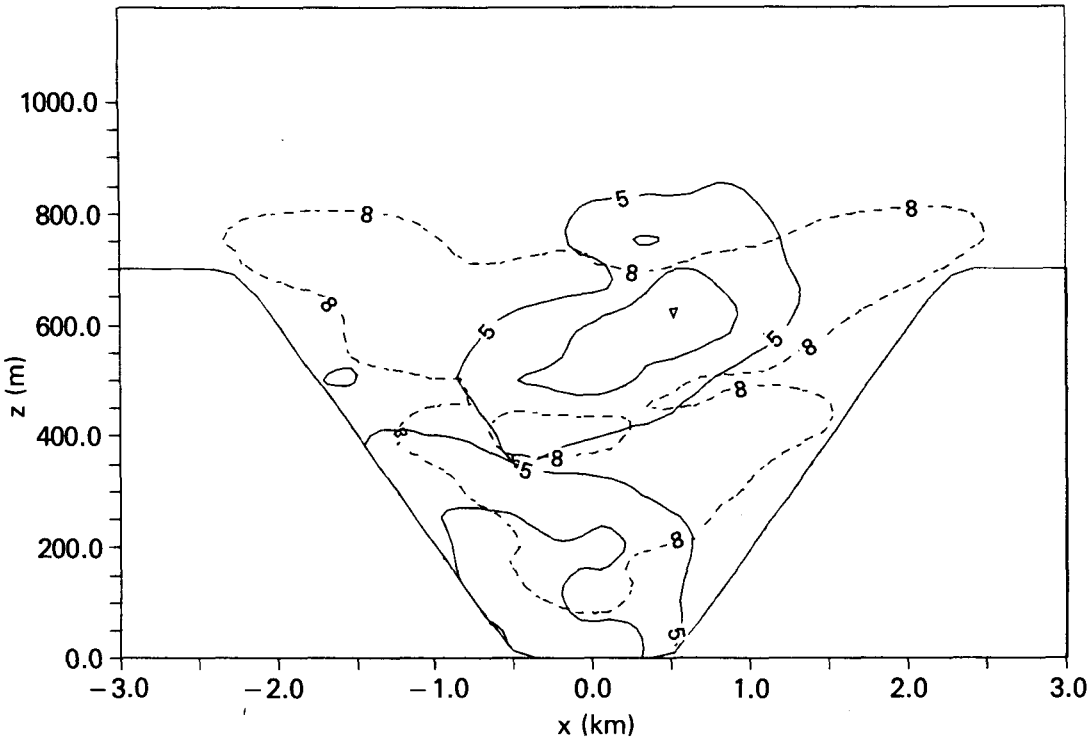


Time = 120 Minutes After Sunrise

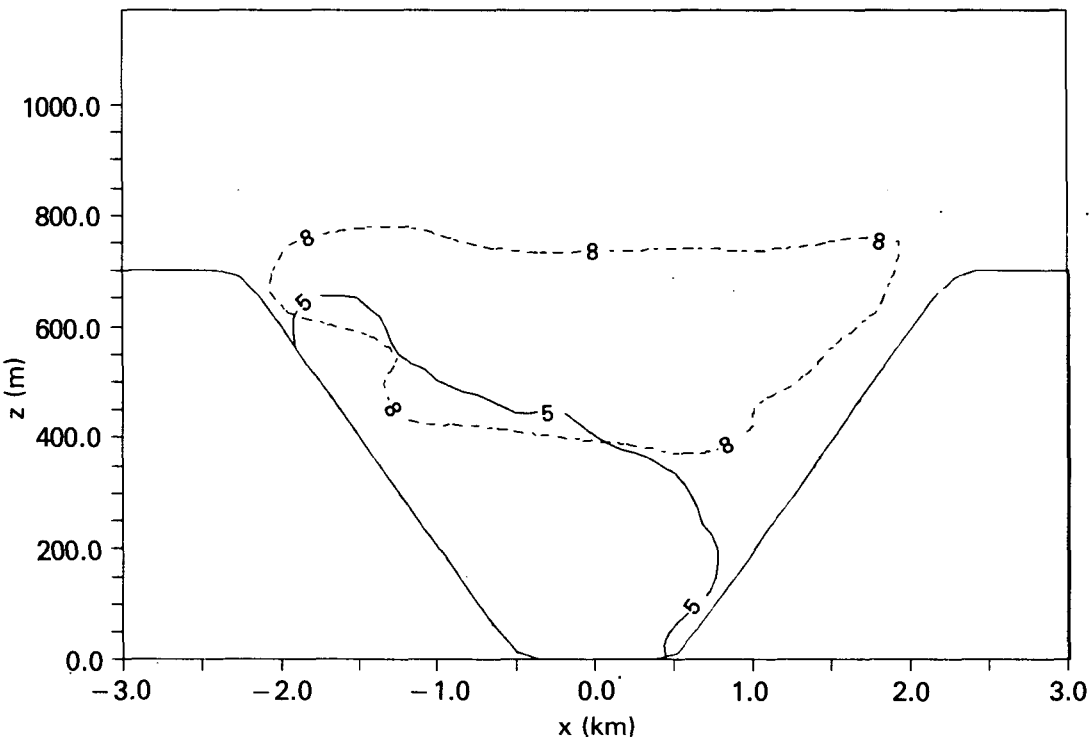


Time = 180 Minutes After Sunrise

FIG. 4. (*Continued*)

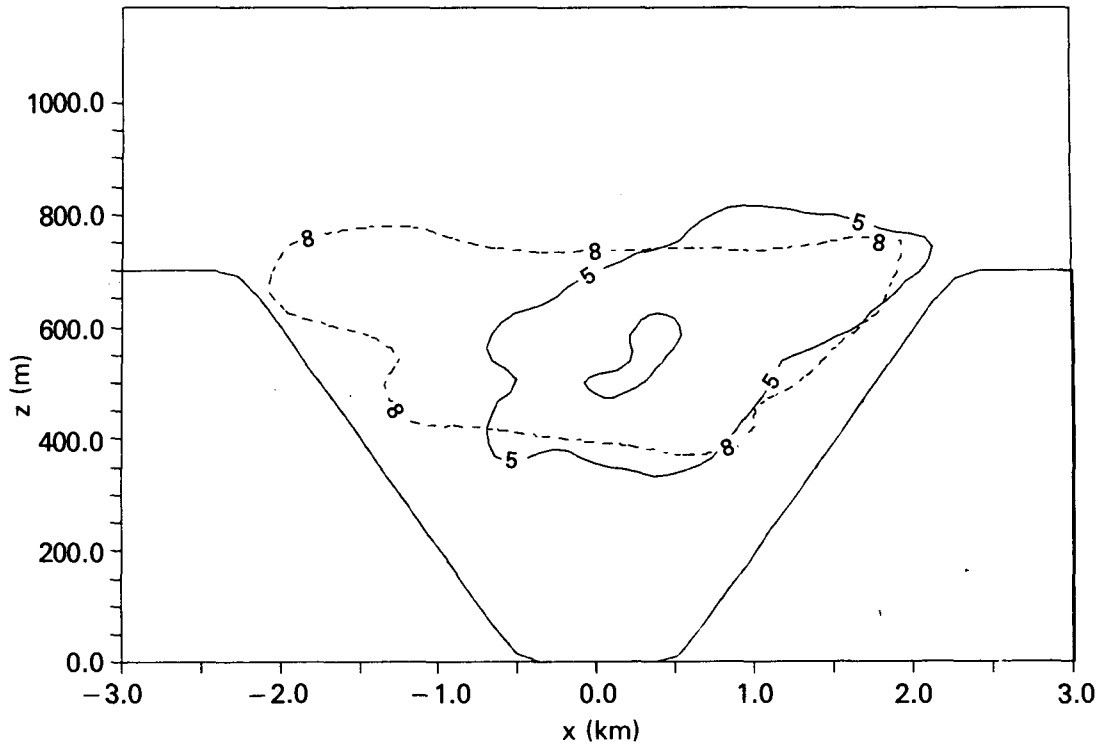


Time = 180 Minutes After Sunrise

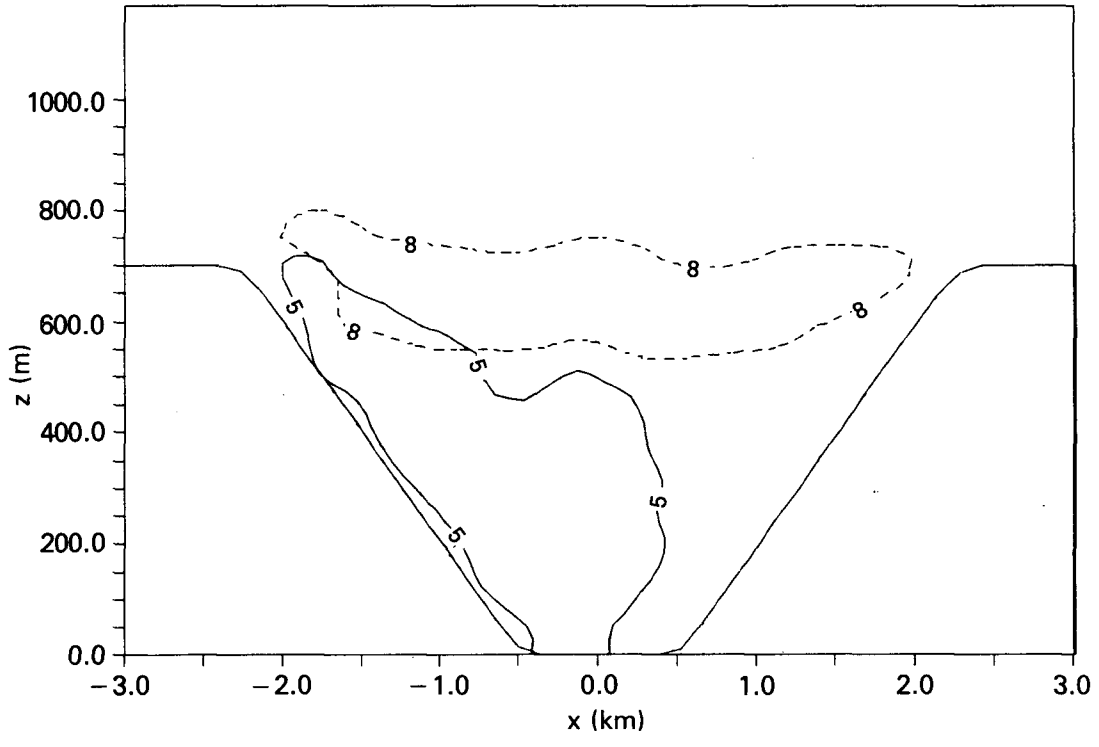


Time = 240 Minutes After Sunrise

FIG. 4. (*Continued*)

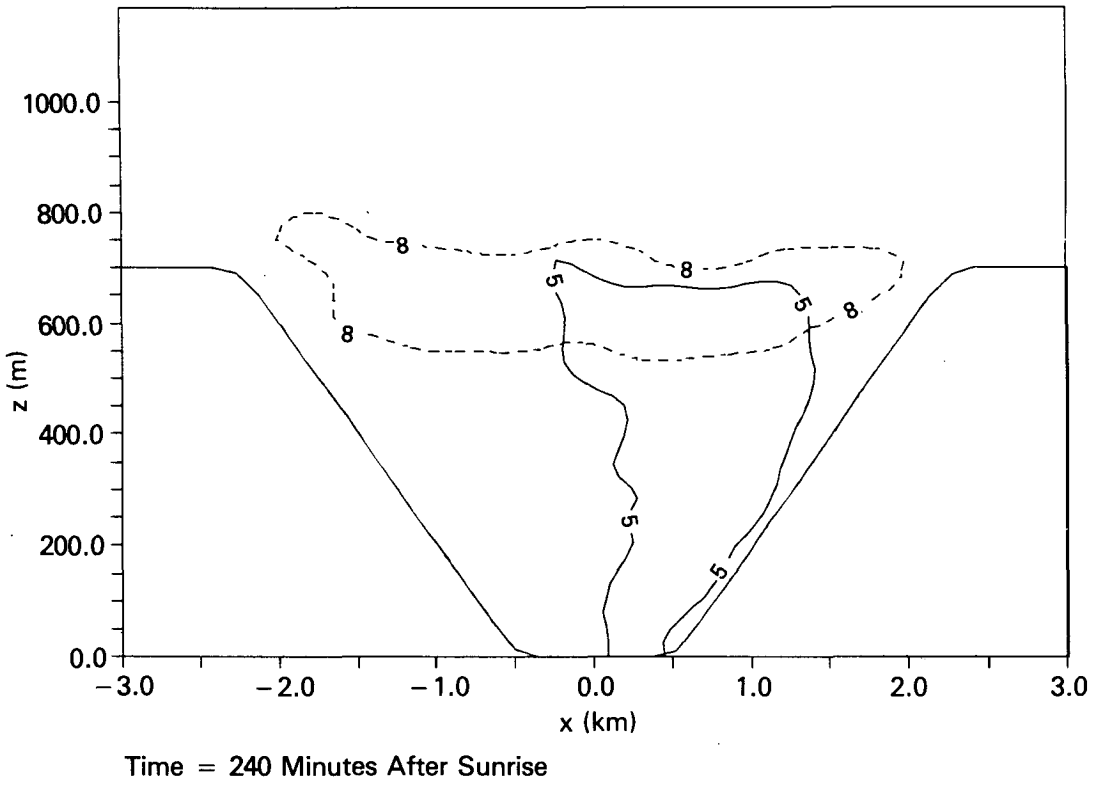


FIG. 4. (*Continued*)

above the valley. The outflow region over the northeast ridge draws air containing material from the upper plume over the ridgecrest, distorting the plume shape, although the peak concentrations are still found above the valley axis. Four hours after sunrise, only a thin remnant of the stable layer remains at ridgetop elevation (Fig. 4f and 4g). Both plumes were well dispersed at this time as the growing CBL entrained the upper plume and mixed it through the valley boundary layer. It is interesting to note that while concentrations of material from the lower plume were higher in the southwest half of the valley, concentrations of material in the upper plume were higher in the northeast half of the valley.

### *b. Winter case results*

In the winter case, the northeast sidewall remained shaded for only 30 min after sunrise, a period when the heating over the southwest slope was weak. In contrast to the summer case, the lower plume shifts only slightly toward the southwest sidewall by 90 min after the start of the simulation (Fig. 6a). The upper plume is much less distorted and the peak concentrations in both plumes are higher than were seen in the summer run. By 2 h after sunrise (Fig. 6b), growth of the CBL and its associated rapid mixing have significantly reduced the peak concentration of the lower plume as it fumigates the region over the valley floor. The upper plume has retained its structure in the stable region aloft with its weak dispersion characteristics and diminished cross-valley circulations.

An hour later (Fig. 6c and 6d), the intensity of the cross-valley circulations had increased and enhanced the lateral mixing of the upper plume, although there was no tendency to favor advection toward either ridge as in the summer case. The lower plume was symmetrically well mixed through the valley CBL and the thermodynamic structure of the stable core exhibited the alternating stability regions over the upper sidewalls. Four hours after sunrise (Fig. 6e and 6f), the lower section of the upper plume was entrained by strong eddies in the growing CBL, which have produced a small potential temperature "jump" typical of convective layers over flat terrain in the remnants of the nocturnal stable layer. A 2.0 m $s^{-1}$ updraft region over the valley center distorts the upper plume structure. Upslope wind speeds range from 0.4 m $s^{-1}$ at elevations 200 m above the floor to 2.0 m $s^{-1}$ at ridgetop. These winds vent tracer material from both plumes to the overlying neutral layer. Near the base of the sidewalls, the winds actually blow downslope to feed the convective updraft over the valley floor.

### *c. Analysis of results*

The differences between the results of the two simulations as well as the differences in dispersion char-

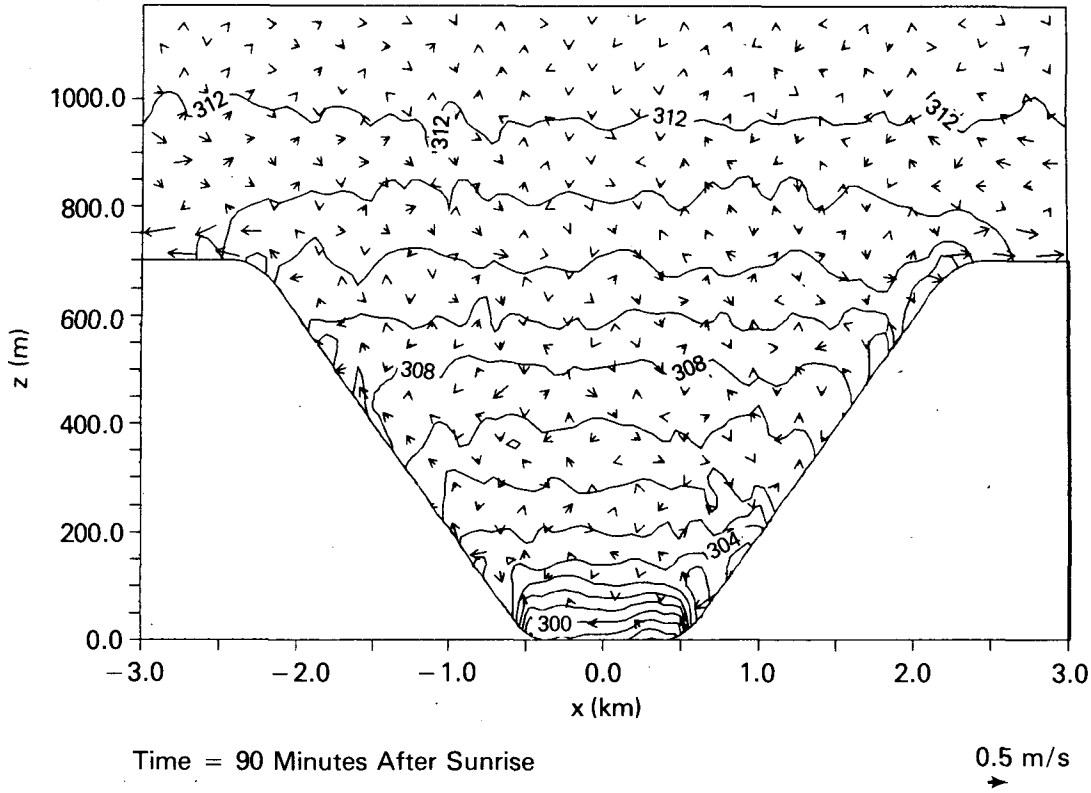


FIG. 5. Wind and potential temperature structure for summer case after 90 min. Contour interval is 1 K.

acteristics between the two plumes in each simulation reveal a great deal of information about dispersion in narrow valleys. In the summer case, the lower plume dispersed in much the same manner as the real plume observed in Brush Creek. The plume drifted toward the heated southwest sidewall while the northeast sidewall was still shaded. It later became entrained in the growing CBL over the lower slope and material was advected up the sidewall in the slope wind. The more elevated plume, however, behaved quite differently than the lower one. Since it remained in the stable layer longer, it diffused more slowly and became distorted by the cross-valley circulations induced by the differences in surface heating between the two sidewalls. Despite the asymmetry in the mass flow field, the thermodynamic structure of the valley boundary layer remained symmetric through the morning. As was seen in earlier studies, cross-valley mixing and internal gravity waves propagating through the stable region counteract the asymmetry in surface heating between the two opposing sidewalls. The drift of the upper plume toward the more weakly heated side was a consequence of the strong outflow region over the ridge pulling air of the same potential temperature from the valley center to satisfy mass continuity. Over the opposite sidewall, stronger heating induced a more vigorous slope wind to feed the outflow circulation with less mass compensation required by air flowing from the valley center. This effect is exaggerated by the idealized nature of the model topography. In real valleys, there is seldom a flat ridge at the sidewell crest, but rather a gradual decrease in slope angle with elevation. The flat plateau region in the model forms a small-scale thermal low pressure region that is much stronger than those that would be observed.

Since the difference in surface heating rate between the sidewalls in winter was much less than that found in the summer, plume dispersion was nearly symmetric in the winter simulation. Two hours after sunrise, the lower plume became well mixed in the growing CBL and slope winds over both sidewalls vented material to the neutral layer above the valley. Late in the morning, the upper plume also dispersed symmetrically in the CBL. The destruction of the nocturnal stable layer proceeded more slowly than that in the summer case because the total heating rate of the valley atmosphere was less. Little inversion descent was observed in either case because the high heating rate over the lower valley surfaces coupled with the weak stability of the valley atmosphere promotes the development of a rapidly growing CBL. Under different circumstances, however, especially when snow covers the valley surfaces, stable layer subsidence may be more important in plume dispersion.

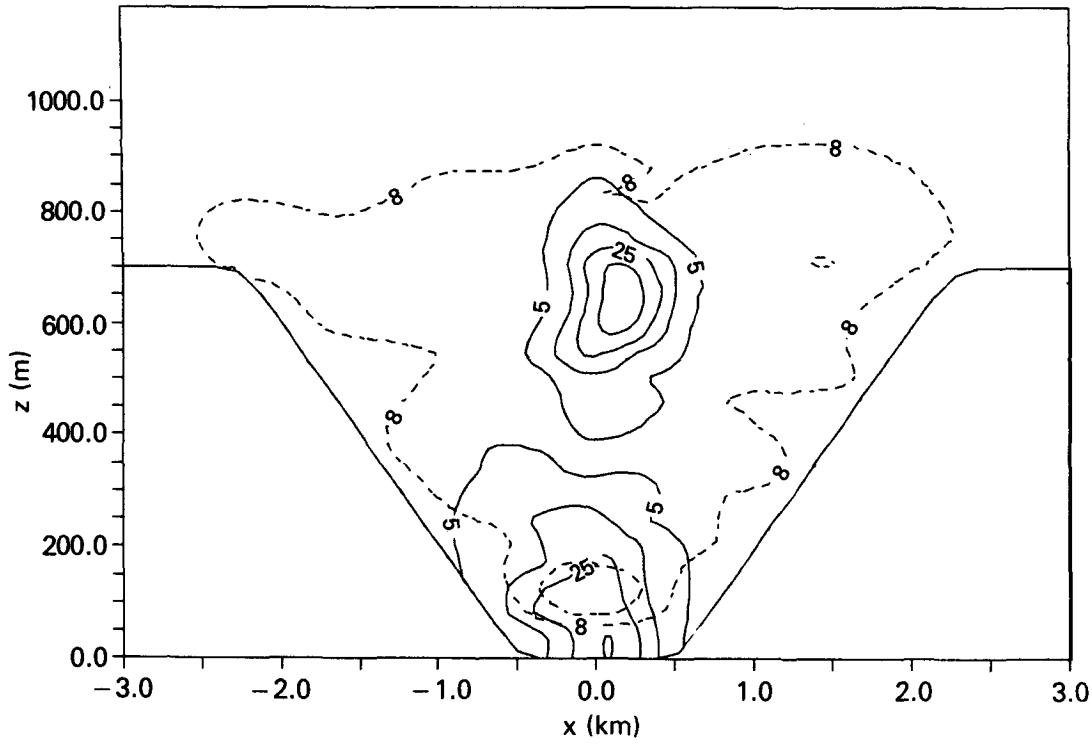


Time = 90 Minutes After Sunrise

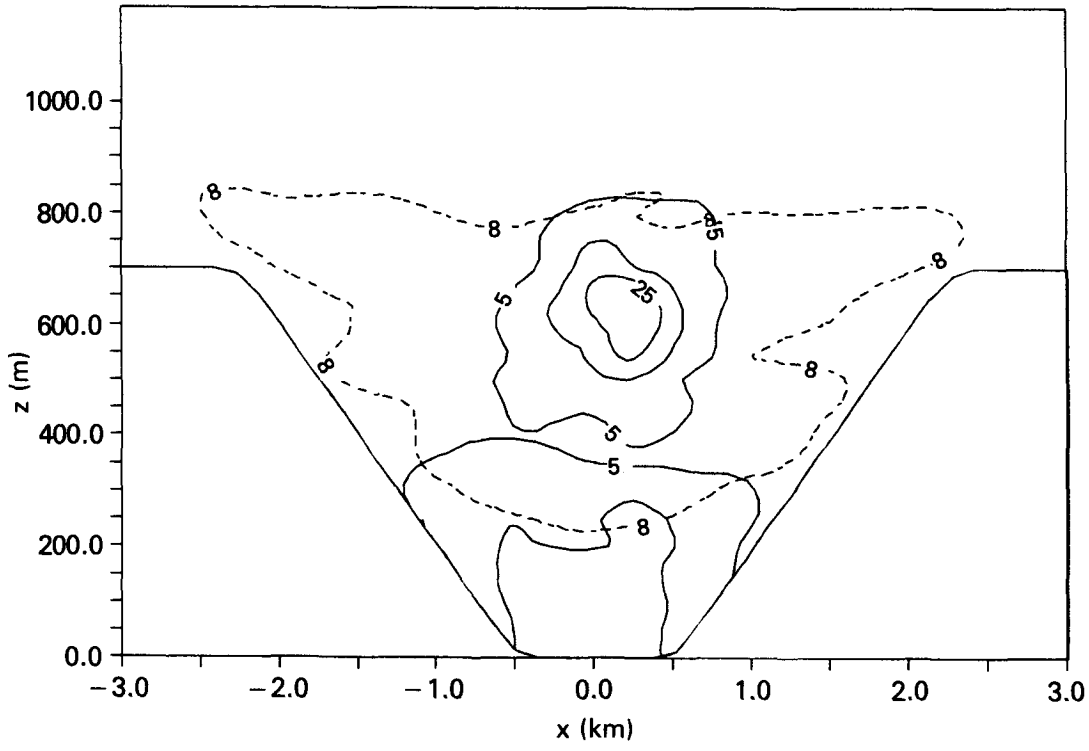


Time = 120 Minutes After Sunrise

FIG. 6. Plume structure (solid contours) and lapse rate (dashed contours) for winter case after (a) 90 min, (b) 120 min, (c) 180 min for lower plume, (d) 180 min for upper plume, (e) 240 min for lower plume, and (f) 240 min for upper plume.

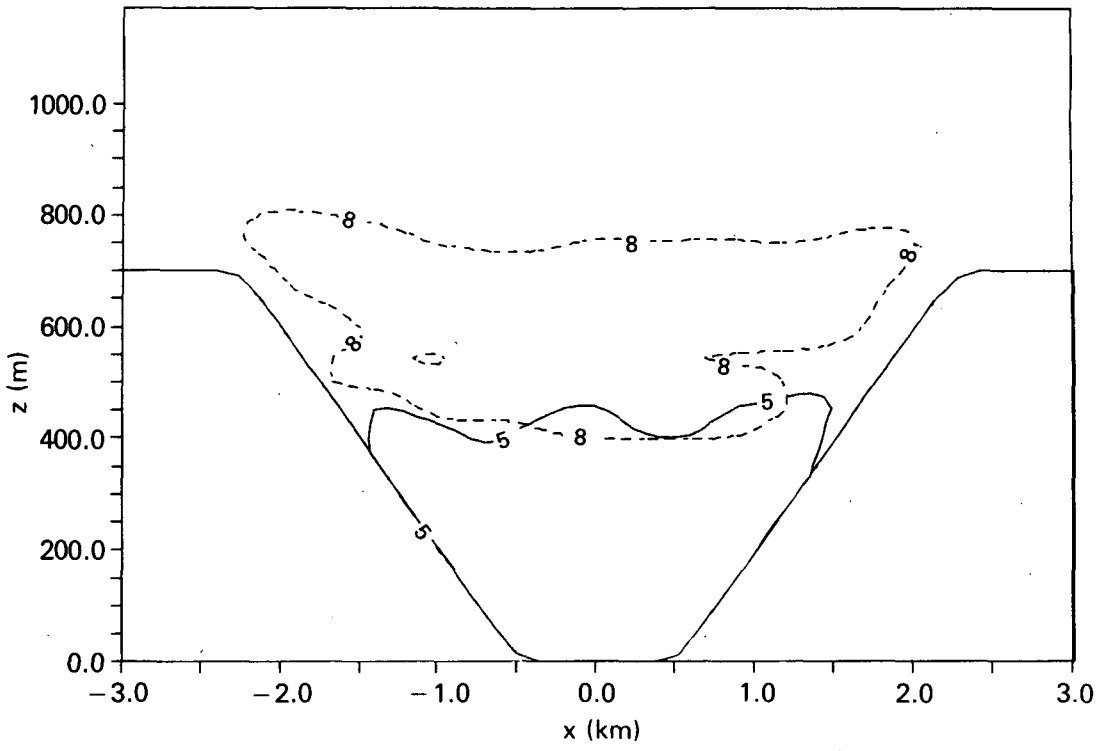


Time = 180 Minutes After Sunrise

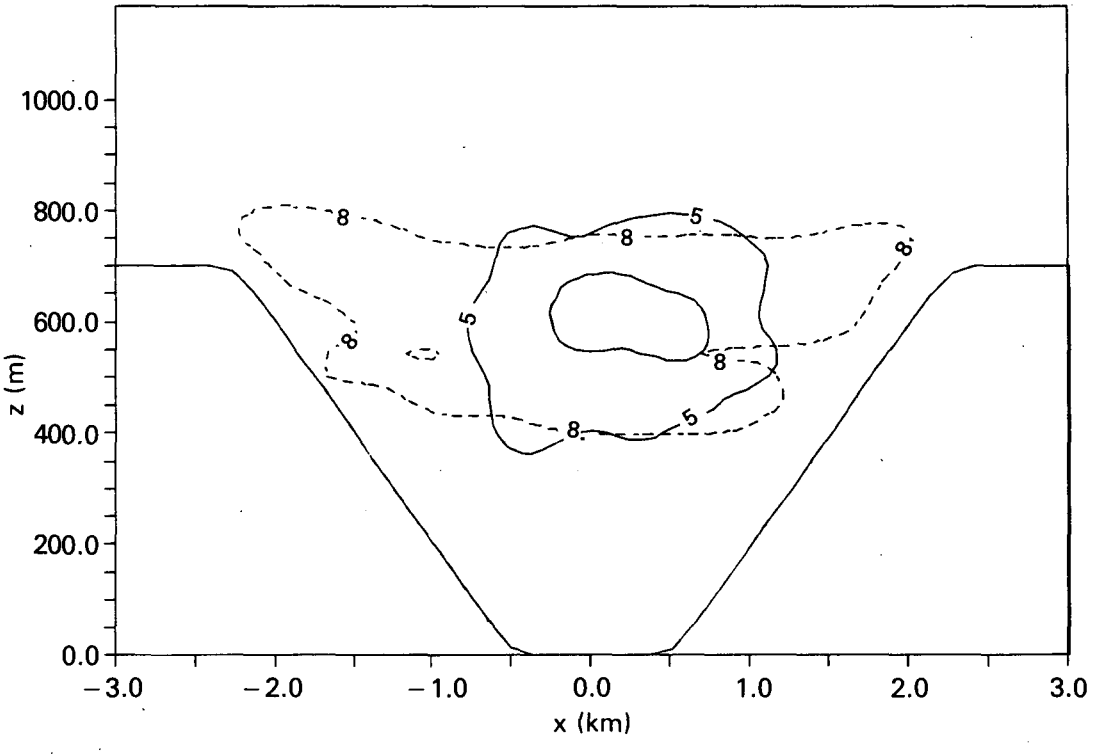


Time = 180 Minutes After Sunrise

FIG. 6. (*Continued*)

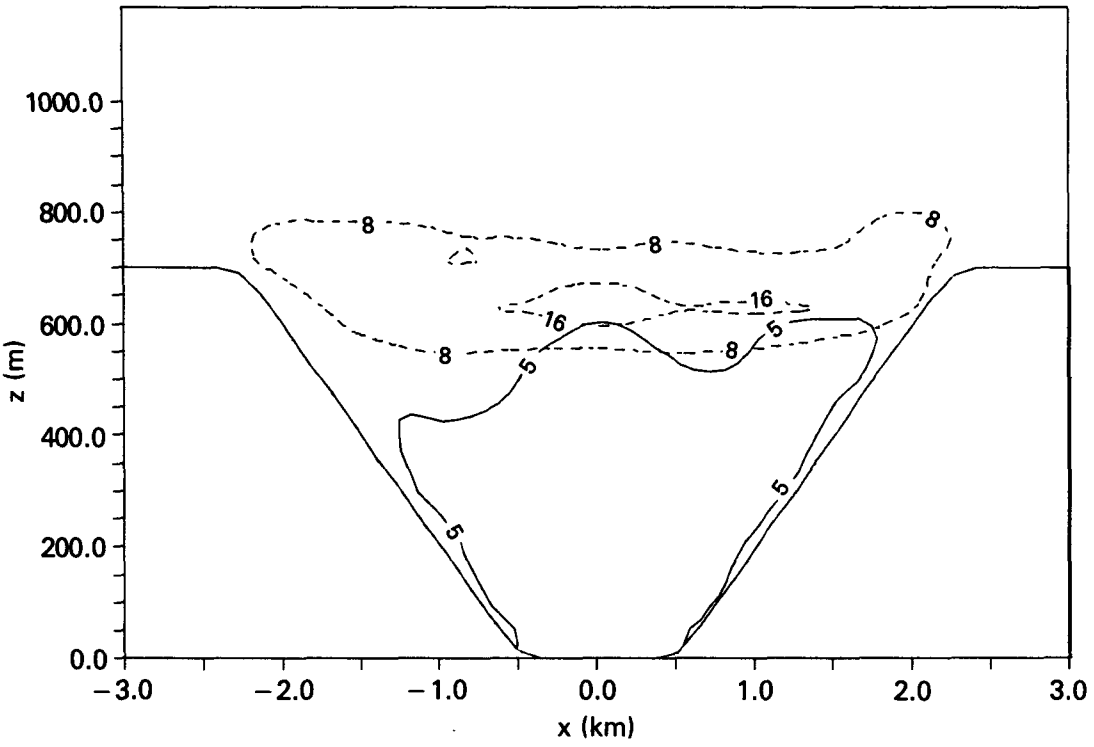


Time = 240 Minutes After Sunrise

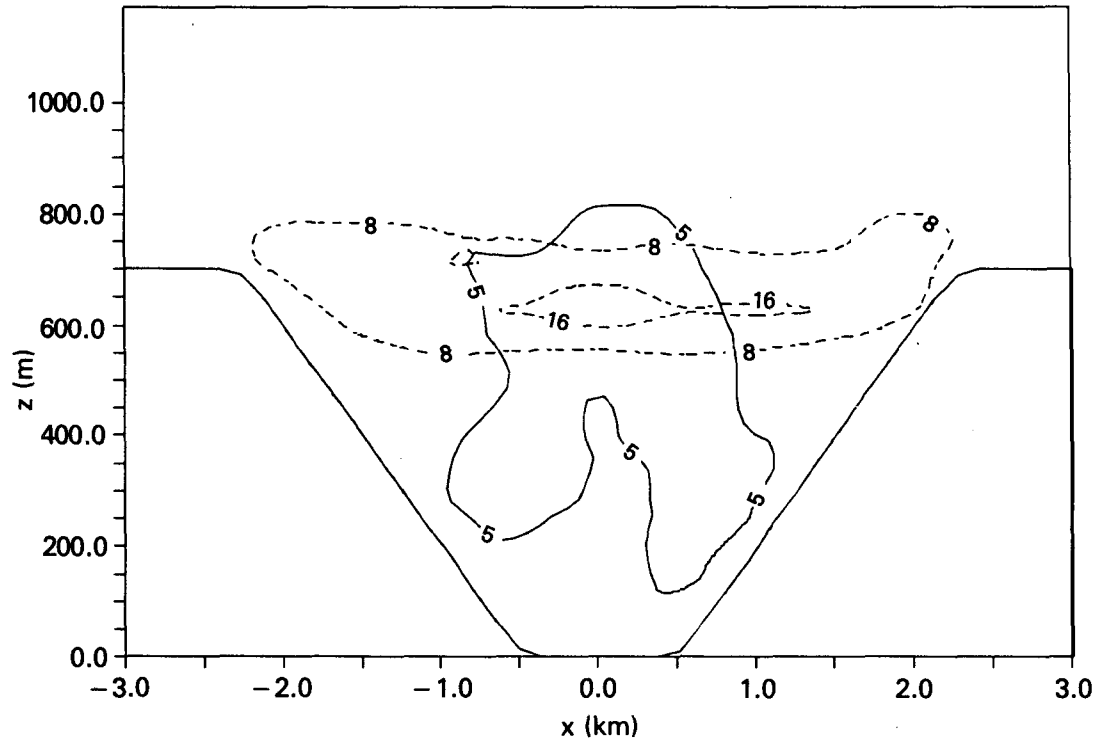


Time = 240 Minutes After Sunrise

FIG. 6. (*Continued*)

## 5. Conclusions

These simulations reveal that plume dispersion in narrow mountain valleys is strongly dependent on source elevation and surface heating distribution. The boundary layer transition period in both simulations was dominated by CBL growth with very limited inversion descent. In the summer case, the lower plume migrates to the more strongly heated sidewall during the first 90 min after sunrise. Thereafter, the tracer material was advected up the slope in a turbulent 0.5–2.0 m $s^{-1}$ slope flow. These results are consistent with observations of plume dispersion taken during the 1982 ASCOT field experiments. At the same time, the upper plume dispersed slowly in the elevated remnants of the nocturnal stable layer. Three to four hours after sunrise, the upper plume was fumigated through the depth of the valley when it was entrained by the growing CBL. By contrast, both plumes were dispersed evenly through the growing CBL after their entrainment in the winter simulation when the difference in heating rates was much less. The thermal structure of the boundary layer in both simulations remained nearly symmetric about the valley axis. Mean flow structure in a boundary layer dominated by small-scale waves and turbulent motions is difficult to determine without high time resolution statistical analysis or the use of tracer materials, as was doen here. The lateral diffusion of the elevated plumes while they were still in the stable layer was much greater than the vertical diffusion because of mixing induced by the small-scale cross-valley processes. This effect has been observed in other studies of mountain-valley dispersion (Start et al. 1975).

In future work, these simulations will be extended to three dimensions to include the effect of the along-valley wind reversal on dispersion. The results of this study also demonstrate the need to conduct field experiments in a variety of conditions, including wintertime cases with snow covered surfaces. Earlier model results (Bader and McKee 1985) suggest that ambient wind, variable surface albedo and surface moisture have been demonstrated to affect boundary layer development. Therefore, their effects on the dispersion characteristics of plumes in valley environments should also be examined.

*Acknowledgments.* This work was funded by the U.S. Department of Energy under contract DE-AC06-76RLO 1830. Numerical model simulations were performed at the National Magnetic Fusion Energy Computer Center, which is supported by the DOE Office of Energy Research.

REFERENCES

Bader, D. C., and T. B. McKee, 1983: Dynamical model simulation of the morning boundary layer development in deep mountain valleys. *J. Climate Appl. Meteor.*, **22**, 341–351.

——, and ——, 1985: Effects of shear, stability and valley characteristics on the destruction of temperature inversion. *J. Climate Appl. Meteor.*, **24**, 822–832.

——, —— and G. J. Tripoli, 1987: Mesoscale boundary layer evolution over complex terrain. Part I: Numerical simulation of the diurnal cycle. *J. Atmos. Sci.*, **44**, 2824–2838.

Businger, J. A., J. D. Wyngaard, Y. Izumi and E. F. Bradley, 1971: Flux profile relationships in the atmospheric surface layer. *J. Atmos. Sci.*, **28**, 181–189.

Clark, T. L., 1977: A small-scale dynamic model using a terrain following coordinate transformation. *J. Comput. Phys.*, **24**, 196–215.

Klemp, J. B., and D. R. Durran, 1983: An upper boundary condition permitting internal gravity wave radiation in numerical mesoscale models. *Mon. Wea. Rev.*, **111**, 430–444.

Louis, J., 1979: A parametric model of vertical eddy fluxes in the atmosphere. *Bound.-Layer Meteor.*, **17**, 187–202.

Orlanski, I., 1976: A simple boundary condition for unbounded hyperbolic flows. *J. Comput. Phys.*, **21**, 251–269.

Revfeim, K. J. A., 1976: Solar radiation at the site of known orientation on the earth's surface. *J. Appl. Meteor.*, **15**, 651–656.

Start, G. E., C. R. Dickson and L. L. Wendell, 1975: Diffusion in a canyon within rough mountainous terrain. *J. Appl. Meteor.*, **14**, 333–346.

Tripoli, G. J., and W. R. Cotton, 1982: The Colorado State University three-dimensional cloud/mesoscale model—1981. Part 1: General theoretical framework and sensitivity experiments. *J. Rech. Atmos.*, **16**, 185–219.

Whiteman, C. D., 1982: Breakup of temperature inversions in deep mountain valleys. Part I: Observations. *J. Appl. Meteor.*, **21**, 270–289.

——, 1989: Morning transition tracer experiments in a deep narrow valley. *J. Appl. Meteor*, **28**, 626–635.

——, and T. B. McKee, 1982: Breakup of temperature inversions in complex terrain. Part 2: Thermodynamic model. *J. Appl. Meteor.*, **21**, 290–302.

——, and K. J. Allwine, 1985: VALMET—A Valley Air Pollution Model. PNL-4728 Rev. 1, Pacific Northwest Lab., Richland, WA, 176 pp.

Yamada, T., 1983: Simulations of nocturnal drainage flow by a $q^2 - l$ turbulence closure model. *J. Atmos. Sci.*, **40**, 91–106.